circle radii to points Q_2 and Q_1, as shown in Fig. 2. As mentioned previously, these angles α_0 and β_0 are the correct values of α and β if $\theta \leq \pi$ and $t_F \leq t_m$. If $\theta > \pi$, $\beta = -\beta_0$ and if $t_F > t_m$, $\alpha = 2\pi - \alpha_0$, all of which can be interpreted geometrically in Fig. 2.

The distance d from point P_2 to the rectilinear center R is easily found to be $s-a$ using the fact that $P_1F_R = s-c$ and $P_2F_R^* = 2a-s$. Thus, the center of the auxiliary circle R can be located relative to point P_2 without explicit determination of the location of the rectilinear foci. The geometrical construction is then summarized as follows:

1) Construct a circle of radius a centered at point R a distance $d = s-a$ from P_2. (If $0 \leq d \leq c$, point R lies on the chord; if $d<0$, it lies on the extension of the chord through point P_2; if $d>c$, it lies on the extension of the chord through point P_1.)

2) Construct the two lines normal to the chord through points P_1 and P_2, intersecting the circle at points Q_1 and Q_2.

3) Construct the lines from point R to points Q_1 and Q_2. These lines form the angles β_0 and α_0 with the chord.

Two special cases can be identified in Fig. 2. For the minimum-energy ellipse between P_1 and P_2, $a = a_m = s/2$, points P_2 and F_R^* are coincident, and $\alpha_0 = \pi$. The case in which the rectilinear center R lies at the midpoint of the chord ($d = c/2$) is the symmetric ellipse,[2,4] the ellipse of smallest eccentricity connecting points P_1 and P_2.

It is interesting to note that in Fig. 2 the difference in the values of eccentric anomaly $E_2 - E_1$ on the *original* elliptical path between points P_1 and P_2 can be identified as an angle, using the fact[4,5] that $\alpha - \beta = E_2 - E_1$. The value of $E_2 - E_1$ shown in Fig. 2 is for the case $\theta \leq \pi$, $t_F \leq t_m$. For the other possible cases, $E_2 - E_1$ can also be geometrically interpreted as an angle in Fig. 2.

Hyperbolic Orbits

For hyperbolic orbits, the angles γ and δ are the analogs of α and β and the time-of-flight equation is[2]

$$\sqrt{\mu}\, t_F = a^{3/2}\left[(\sinh\gamma - \sinh\delta) - (\gamma - \delta)\right] \tag{5}$$

where $\sinh(\gamma/2)$ and $\sinh(\delta/2)$ are equal to the right-hand sides of Eqs. (2) and (3), respectively. In Eq. (5), δ is replaced by its negative if $\theta > \pi$.

Kepler's equation for a hyperbolic orbit expressed in terms of hyperbolic-eccentric anomaly H is

$$\sqrt{\mu}\, t_F = a^{3/2}\left[e(\sinh H_2 - \sinh H_1) - (H_2 - H_1)\right] \tag{6}$$

Thus, the angles γ and δ can be interpreted as the values of hyperbolic-eccentric anomaly H_2 and H_1 on the rectilinear hyperbola ($e=1$) between points P_1 and P_2, having the same values of $r_1 + r_2$ and a as the original orbit.

Since the hyperbolic-eccentric anomaly H does not have a geometrical interpretation as an angle, it is convenient to employ the Gudermannian transformation[6,7] from hyperbolic to trigonometric functions $\sinh H = \tan\zeta$, for which $H = \log\tan(\zeta/2 + \pi/4)$. The values of the Gudermannian angles ζ_1 and ζ_2 corresponding to H_1 and H_2 can be interpreted geometrically, using the rectilinear hyperbola in terms of the tangent lines from P_1 and P_2 to the auxiliary circle of radius a centered at R, as shown in Fig. 3. The distance d from R to P_2 is $s+a$ and the angles γ and δ are given by

$$\begin{aligned} \gamma &= \log\tan(\zeta_2/2 + \pi/4) \\ \delta &= \log\tan(\zeta_1/2 + \pi/4) \end{aligned} \tag{7}$$

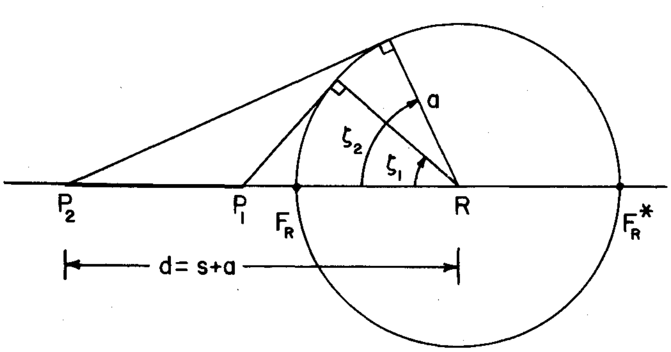

Fig. 3 Interpretation of the angles ζ_1 and ζ_2 for a hyperbolic orbit.

References

[1] Lagrange, J.L., *Oeuvres de Lagrange,* Vol. IV, 1778, p. 559.

[2] Battin, R.H., *Astronautical Guidance,* McGraw-Hill, New York, 1964, pp. 70-77.

[3] Battin, R.H., "Orbital Boundary-Value Problems," Preprint 65-29, *Symposium on Unmanned Exploration of the Solar System,* Denver, Colo., 1965.

[4] Battin, R.H., Fill, T.J., and Shepperd, S.W., "A New Transformation Invariant in the Orbital Boundary-Value Problem," *Journal of Guidance and Control,* Vol. 1, Jan.-Feb. 1978, pp. 50-55.

[5] Battin, R.H., "Lambert's Problem Revisited," *AIAA Journal,* Vol. 15, May 1977, pp. 707-713.

[6] Stumpff, K., *Himmelsmechanik,* VES Verlag, Berlin, 1959, p. 106.

[7] Ehricke, K., *Spaceflight,* Vol. I, Van Nostrand, Princeton, New Jersey, 1960, p. 318.

Relative Motion of Particles in Coplanar Elliptic Orbits

Terry Berreen*
Monash University, Clayton, Victoria, Australia
and
George Svedt†
The University of Adelaide, South Australia, Australia

Introduction

STUDIES of the relative motion of particles in elliptic orbits were primarily prompted by interest in the rendezvous maneuver between an unpowered ferry vehicle and a target satellite in orbit. The relative motion is determined with reference to a coordinate system attached to the target satellite. The purpose of this Note is to expose the need for a simplified solution for coplanar elliptic orbits and to develop and apply such a solution. The results are applicable to any relative motion situation for coplanar orbits such as determining the trajectory of a probe ejected from a space station, rendezvous of orbiting satellites, and the targeting of one space station from another in the same orbital plane.

Brief Survey of Published Solutions

The early solutions, for coplanar orbits and for circular orbits of the target satellite, are obtained from the differential equations of relative motion which are linearized by approximating for small relative displacements. Such solutions are determined by Wheelon,[1] Wolowicz et al.,[2] Spradlin,[3]

Received Feb. 27, 1979.

Index categories: Earth-Orbital Trajectories; Analytical and Numerical Methods; Spacecraft Navigation, Guidance and Flight-Path Control.

*Lecturer, Department of Mechanical Engineering.
†Research Associate; formerly Reader in Civil Engineering.

and Clohessy and Wiltshire.[4] The resulting relative motions of the ferry vehicle are recognized to be trochoids by Wolowicz et al.[2]

Eggleston and Beck,[5] in their study of the positions and velocities of a space station and a ferry vehicle during rendezvous and return, compare this linear solution with a numerical solution of the exact equations of motion. They conclude that the linear solution is only adequate when the bodies are in close proximity and the angular position, initially zero, of the space station is small, usually less than $\pi/2$. Knollman and Pyron[6] use an analog computer to investigate the relative trajectories of objects ejected with low speed from a satellite in circular orbit. The trajectories are described as being approximately prolate epicycloids and prolate hypocycloids. The linear solution is extended by London[7] to include second-order displacement terms and he gives two examples to illustrate the greater application of his quadratic solution over the linear solution.

Similar approaches are made to the more general problem of the target satellite in an elliptic orbit. First-order displacement terms only are retained in the solution of de Vries[8] for orbits of low eccentricity and by Tschauner and Hempel[9] for orbits of arbitrary eccentricity. Second-order displacement terms for orbits of low eccentricity are included in the solution of Anthony and Sasaki,[10] and for orbits of arbitrary eccentricity by Euler and Shulman.[11] The latter conclude from their examples that, while the linear solution is adequate for small relative displacements, a numerical solution should be used when many revolutions of the target satellite, or large relative displacements, are involved.

All the above solutions have used the differential equations of relative motion rather than seeking a solution through the known orbital motions. A computational technique, using vector subtraction of the individual orbital motions, to determine accurately the relative motion between two particles in elliptic orbits is given by Lancaster.[12] Eades[13] studies the motion of an orbiting satellite relative to another in a circular orbit and presents linear and quadratic solutions, a numerical solution, and an exact analytic solution for the special case of both satellites having the same orbital period. He confirms the findings of earlier workers that the quadratic solution maintains accuracy to within a few percent for up to two orbital periods, whereas a similar loss of accuracy is suffered by the linear solution in approximately half a period. A paper by Eades and Drewry[14] is given to the special case of one particle in a circular orbit and both particles having the same orbital period.

Berreen and Crisp[15] in considering the trajectories of a probe ejected into an elliptic orbit in the orbital plane of a space station in circular orbit derive an exact analytical solution by transformation of the orbital equations to rotating coordinates. A first-order solution is derived from this exact solution by approximating for low ejection speed. This has an advantage over the earlier linear solution in that no restriction is placed on the relative displacement since there is no secular accumulation of error and the solution osculates with the exact solution at points corresponding to perigee and apogee of the probe's orbit. A geometrical description of these low ejection speed trajectories exposes them as prolate cycloids when plotted in a circular curvilinear coordinate system.

The procedure of Lancaster[12] is the most general for determining particular relative motions. The number of steps obscures the mechanics, however, making it unsuitable for analysis, and so it offers few insights or generalizations into the nature and geometry of the trajectories. There is an obvious need in the classification and prediction of trajectory types for the solution to be in a form which lends itself to analysis. This has been achieved for coplanar trajectories arising from one of the particles being in a circular orbit by the Berreen[16] solution and this Note is to present such a solution for both particles being in coplanar elliptic orbits.

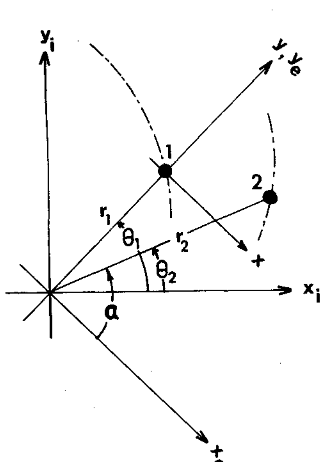

Fig. 1 The coordinate systems.

Coordinate Systems and Orbital Elements

The coordinate systems used to view the motions are shown in Fig. 1, with the two particles in coplanar elliptic orbits being numbered 1, 2. The rotating x,y system is centered on particle 1 with the y axis always aligned with the radius r_1; the rotating x_e,y_e system is Earth (or force-center) centered so that the y and y_e axes are always aligned. The x_i,y_i system is an inertial system with the fixed position of the x_i axis being the same as that of the y_e axis at zero time. Coordinates r_1,θ_1 and r_2,θ_2 are polar coordinates of the particles in the x_i,y_i system and r_2,α are polar coordinates of particle 2 in the rotating x_e,y_e system.

To facilitate description, the term *orbit* will be used for the path of a particle viewed from the inertial (x_i,y_i) system and the term *trajectory* for a path viewed from a rotating (x,y or x_e,y_e) system.

The elliptic orbits are characterized by the following orbital elements: the eccentricity e, the semilatus rectum p, and the apsidal orientation in the established orbital plane, θ^*. The orbits may be defined by either of the following:

1) Both orbital elements e_1,p_1,θ_1^* and e_2,p_2,θ_2^* are known, together with initial values of the true anomalies β_1 and β_2.

2) The orbital elements e_1,p_1,θ_1^* are known together with the initial position (x_0,y_0) and initial velocity $(\dot{x}_0,\dot{y}_0)$ components of particle 2.

For the latter case, the orbital elements p_2,e_2,θ_2^* are determined using the following relationships, where the zero subscript indicates an initial value:

$$(\beta_1)_0 = -\theta_1^*$$

$$(r_1)_0 = p_1/[1+e_1\cos(\beta_1)_0],\ (r_2)_0^2 = x_0^2 + [y_0 + (r_1)_0]^2$$

$$\sin(\theta_2)_0 = -x_0/(r_2)_0,\ \cos(\theta_2)_0 = [y_0 + (r_1)_0]/(r_2)_0$$

$$(Vr_1)_0 = \sqrt{GM_e}(e_1/\sqrt{p_1})\sin(\beta_1)_0 \qquad (V\theta)_0 = \sqrt{GM_e}\sqrt{p_1}/(r_1)_0$$

$$(Vr_2)_0 = [(Vr_1)_0 + \dot{y}_0]\cos(\theta_2)_0 + [(V\theta_1)_0 - \dot{x}_0]\sin(\theta_2)_0$$

$$(V\theta_2)_0 = [(V\theta_1)_0 - \dot{x}_0]\cos(\theta_2)_0 - [(Vr_1)_0 + \dot{y}_0]\sin(\theta_2)_0$$

Then, using the relationships of Crisp[17]

$$p_2 = [(r_2)_0(V\theta_2)_0]^2/GM_e$$

$$e_2^2 = 1 - p_2\{2/(r_2)_0 - [(Vr_2)_0^2 + (Vr_1)_0^2]/GM_e\}$$

$$\theta_2^* = (\theta_2)_0 - \cos^{-1}\{[p_2 - (r_2)_0]/[e_2(r_2)_0]\}$$

$$\theta_2^* = (\theta_2)_0 - \sin^{-1}[\sqrt{p_2}(Vr_2)_0/(e_1\sqrt{GM_e})]$$

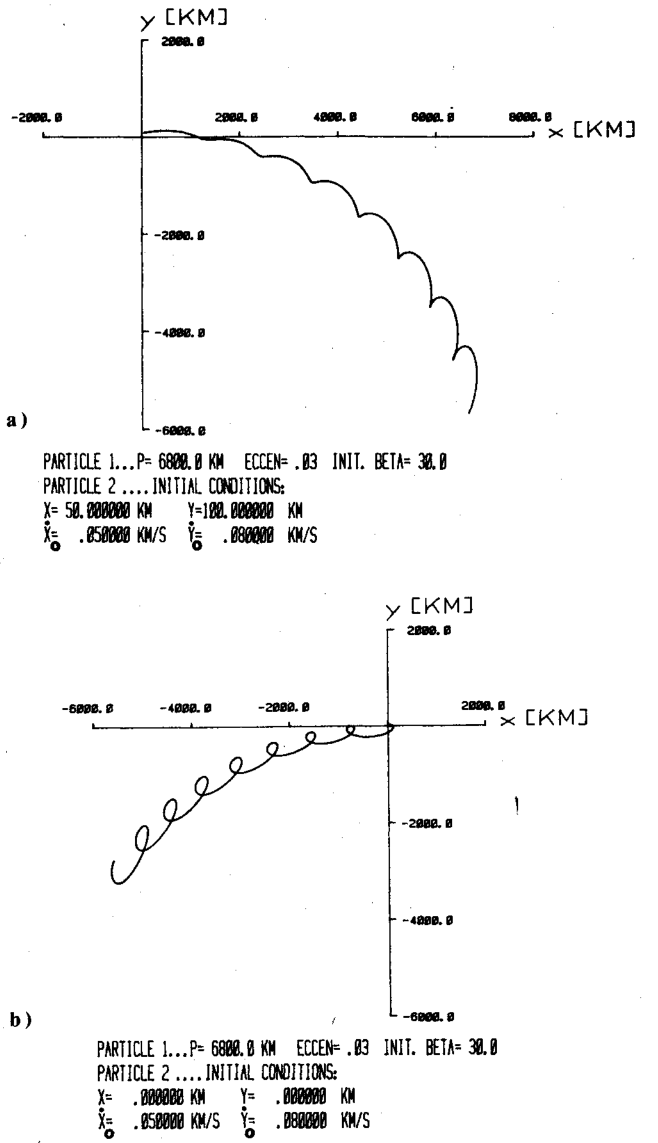

Fig. 2 Trajectories with particle 1 in the same elliptic orbit.

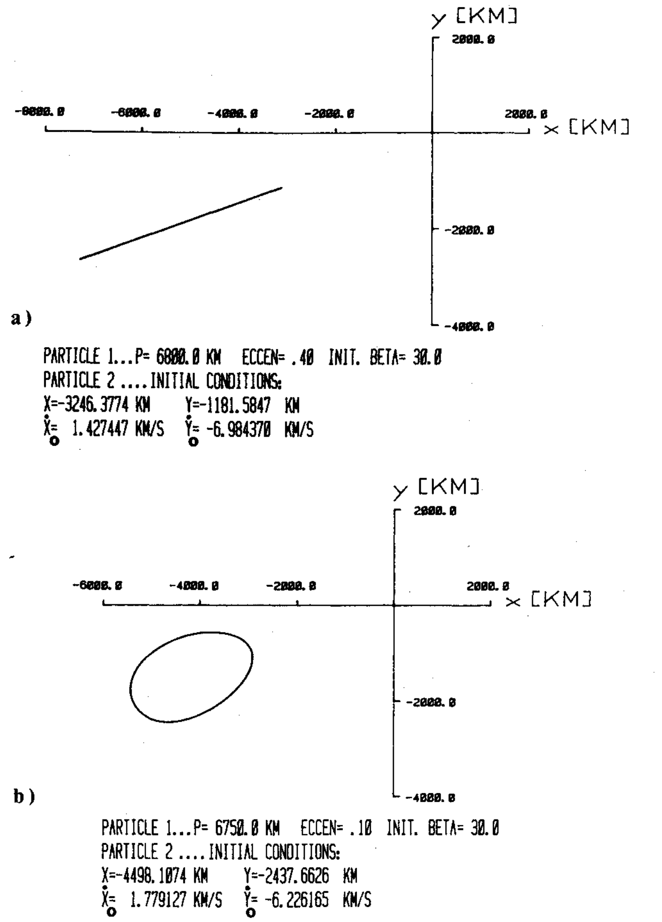

Fig. 3 Periodic trajectories.

G being the universal constant of gravitation, M_e the mass of the Earth, and Vr, $V\theta$ the radial and circumferential velocity components respectively.

Trajectory Determination

The trajectory is determined in polar coordinates r_2,α in the x_e,y_e rotating system from which the coordinates x,y are readily determined. From Fig. 1,

$$\alpha = \pi/2 - (\theta_1 - \theta_2) \tag{1}$$

but θ_1,θ_2 differ from the true anomalies β_1,β_2 by the respective apsidal orientations θ_1^*,θ_2^*, so that

$$\alpha = \pi/2 + \theta_2^* - \theta_1^* + \beta_2 - \beta_1 \tag{2}$$

At a given time t, the eccentric anomalies E_1,E_2 are determined by solving the respective Kepler's Equation

$$n(t - t^*) = E - e\sin E \tag{3}$$

where for each orbit, the mean motion n is obtained from the semimajor axis length a,

$$n^2 = GM_e/a^3 = GM_e(1-e^2)^3/p^3 \tag{4}$$

and t^*, the time of perigee passage, is obtained from Eq. (3) by substituting the initial values $t=0$ and $(\beta_1)_0 = -\theta_1^*$, $(\beta_2)_0 = (\theta_2)_0 - \theta_2^*$. The true and eccentric anomalies are related by

$$\tan\tfrac{1}{2}E = [(1-e)/(1+e)]^{1/2}\tan\tfrac{1}{2}\beta \tag{5}$$

The true anomalies β_1,β_2 at time t are determined using Eq. (5) and r_1,r_2 are given by the respective polar equations

$$r = p/(1 + e\cos\beta) \tag{6}$$

The Cartesian position x,y of particle 2 in the rotating system attached to particle 1 is then

$$x = r_2\cos\alpha \qquad y = r_2\sin\alpha - r_1 \tag{7}$$

Examples and Discussion

Four trajectory examples computed by the above procedure are shown in Figs. 2 and 3. In the two examples of Fig. 2, particle 1 is in the same elliptic orbit and initially at the same position. For Fig. 2a the particles are initially separated; for Fig. 2b they are initially together, so this is an example for ejection of a space probe from a space station in elliptic orbit. The distinct difference between the resulting trajectories for differing initial positions of particle 2 is evident. For Fig. 3a the particles are in orbits having the same values of e and p but differing values of θ^*, and both particles are at the same angular position in their respective orbits. Hence $r_1 = r_2$ and $\beta_1 = \beta_2$, so Eq. (2) becomes

$$\alpha = \pi/2 + \theta_2^* - \theta_1^* \tag{8}$$

and from Eq. (7)

$$y/x = (\sin\alpha - 1)/\cos\alpha \tag{9}$$

so that the trajectory is a straight line segment. For Fig. 3b the orbits have equal periods, so the resulting trajectory is periodic and in this case approximately elliptic.

References

[1] Wheelon, A.D., "Midcourse and Terminal Guidance," *Space Technology*, edited by H. Seifert, Wiley, New York, 1959, Chap. 26.

[2] Wolowicz, C.H., Drake, H.M., and Videan, E.N., "Simulator Investigation of Controls and Display Required for Terminal Phase of Coplanar Orbital Rendezvous," NASA TN D-511, 1960.

[3] Spradlin, L.W., "The Long-Time Satellite Rendezvous Trajectory," *Proceedings of the National Specialist Meeting on Guidance of Aerospace Vehicles*, Boston, Mass., 1960, pp. 21-27.

[4] Clohessy, W.H. and Wiltshire, R.S., "Terminal Guidance System for Satellite Rendezvous," *Journal of the Aerospace Sciences*, Vol. 27, Sept. 1960, pp. 653-658.

[5] Eggleston, J.M. and Beck, H.D., "A Study of the Positions and Velocities of a Space Station and a Ferry Vehicle During Rendezvous and Return," NASA TR R-87, 1961.

[6] Knollman, G.C. and Pyron, B.O., "Relative Trajectories of Objects Ejected from a Near Satellite," *AIAA Journal*, Vol. 1, Feb. 1963, pp. 424-429.

[7] London, H.S., "Second-Approximation to the Solution of Rendezvous Equations," *AIAA Journal*, Vol. 1, July 1963, pp. 1691-1693.

[8] de Vries, J.P., "Elliptic Elements in Terms of Small Increments of Position and Velocity Components," *AIAA Journal*, Vol. 1, Nov. 1963, pp. 2626-2629.

[9] Tschauner, J. and Hempel, P., "Rendezvous zu einem in elliptischer Bahn umlaufenden Ziel," *Astronautica Acta*, Vol. 11, 1965, pp. 104-109.

[10] Anthony, M.L. and Sasaki, F.T., "Rendezvous Problem for Nearly Circular Orbits," *AIAA Journal*, Vol. 3, Sept. 1965, pp. 1666-1673.

[11] Euler, E.A. and Shulman, Y., "Second-Order Solution to the Elliptical Rendezvous Problem," *AIAA Journal*, Vol. 5, May 1967, pp. 1033-1035.

[12] Lancaster, E.R., "Relative Motion of Two Particles in Elliptic Orbits," *AIAA Journal*, Vol. 8, Oct. 1970, pp. 1878-1879.

[13] Eades, J.B. Jr., "Relative Motion of Orbiting Satellites," Analytical Mechanics Associates Inc., Maryland, Rept. 72-77, 1972.

[14] Eades, J.B. Jr. and Drewry, J.W., "Relative Motion of Near Orbiting Satellites," *Celestial Mechanics*, Vol. 7, 1973, pp. 3-30.

[15] Berreen, T.F. and Crisp, J.D.C., "An Exact and a New First-Order Solution for the Relative Trajectories of a Probe Ejected from a Space Station," *Celestial Mechanics*, Vol. 13, 1976, pp. 75-88.

[16] Berreen, T.F., "On the Relative Trajectories of a Probe Ejected From an Orbiting Space Station," Ph.D. Thesis, Monash University, Australia, Chap. 3.

[17] Crisp, J.D.C., "The Dynamics of Supercircular Multipass Atmospheric Braking," *Astronautica Acta*, VIII, 1962, pp. 1-27.

Technical Comments

Comment on "Active Flutter Control Using Generalized Unsteady Aerodynamic Theory"

Ranjan Vepa*
National Aeronautical Laboratory, Bangalore, India

RECENTLY Edwards et al.[1] published a method for active flutter control and finite state modelling of aeroelastic systems. While this method is extremely good for two-dimensional airfoils in incompressible and supersonic flow, it is not clear exactly how useful it is in subsonic flow and for three-dimensional lifting surfaces. In the latter case explicit solutions for the pressure and airloads in the complex frequency domain are not available, and the construction of these solutions numerically is not an easy matter. To understand this, one must view the contribution of Ref. 1 in perspective, without all the mathematical trimmings.

In general, the aeroelastic equations in the complex frequency domain are usually written as

$$[MS^2 + CS + K + Q(S)]q = 0 \tag{1}$$

In the method presented in Ref. 2, $Q(S)$ is modelled by rational transfer functions, and this contributes additional states to the finite-state model. On the other hand, these are computed from well-known results for simple harmonic motion of the lifting surface.

In Ref. 1, $Q(S)$ is, in principle, approximated by a polynomial in S; that is

$$Q(S) = P_0 S^2 + P_1 S + P_2$$

where $P_0 = 0$ for Mach number $\neq 0$, such that the eigenvalues and eigenvectors of the system of coupled equations,

$$[(M+P_0)S^2 + (C+P_1)S + (K+P_2)]q = 0 \tag{2}$$

are identical to those of Eq. (1). This involves the solution of the eigenvalue problem given by Eq. (1), which of course implies that $Q(S)$ must be valid for all S. Thus, in order to construct a finite-state model by the method of Ref. 1, one must not only have calculated the generalized airloads for arbitrary values of the complex frequency S but also solve the complex eigenvalue problem of Eq. (1).

The computation of the unsteady generalized airloads, $Q(S)$, for arbitrary S poses several computational problems and is not an easy task as is assumed in Ref. 1. Furthermore, in order to solve the eigenvalue problem defined by Eq. (1) one must employ fairly sophisticated search techniques.

For three-dimensional lifting surfaces the behavior of the singular induced downwash distributions in the entire complex plane, and not just along the frequency axis, is not clearly known. This problem does not arise for airfoils in incompressible and supersonic flow, which are the only two cases dealt with explicitly in Ref. 1. Thus, in order to extend the unsteady aerodynamics for lifting surfaces in the complex frequency domain, one should first show that singular downwash distributions due to singularities in the unsteady kernel function are uniformly valid in the entire complex plane. Then it is necessary to establish the convergence of the solutions for the pressure to the physically valid solutions just as in the case of numerical methods for solving the lifting surface problem for simple harmonic motions. In the

Received March 2, 1979.

Index categories: Aeroelasticity and Hydroelasticity; Guidance and Control.

*Scientist, Structures Division.